Effective electrons and angular oscillations in quasi-one-dimensional conductors

I. J. Lee* and M. J. Naughton†
Departments of Physics and Chemistry, State University of New York, Buffalo, New York 14260-1500
(Received 15 December 1997)

We show via calculation and experiment that a recently observed angular magnetoresistance effect in low-dimensional conductors can be explained by ''effective electrons,'' which dominate the conductivity for magnetic-field orientations near inflection points on a warped Fermi surface. Closed orbits, which form in certain field orientations, play an insignificant role. In studies of the quasi-one-dimensional molecular metal $(TMTSF)_2PF_6$, we observe, in addition to sharp kink structure of the effect, a series of strong angular oscillations that we ascribe to the Lebed' commensurability resonance (magic angle) effect. [S0163-1829(98)03113-0]

The relative high crystalline purity of molecular organic conductors has led to the synthesis of numerous new materials in which to study the physics and chemistry of electrons in low dimensions. For materials classified as quasi-one-dimensional, a plenitude of new phenomena has been discovered, including recent evidence for unusual superconductivity.[1] Among these are a diversity of angular magnetoresistance oscillation (AMRO) effects, the first of which was the Lebed' magic angle effect[2] discovered in the molecular metal $(TMTSF)_2ClO_4$.[3,4] There have been many proposed explanations of the b-c plane Lebed' effect, including some involving interactions between electrons. They have been modeled in semiclassical calculations with some success, but only after the inclusion of a dubious hopping term.[5] Later, a second resonance effect was discovered in $(TMTSF)_2ClO_4$, attributed to details of the warped, open Fermi surface.[6] This a-c plane effect allows one to accurately measure the transfer integral ratio t_a/t_b in this system, once the Fermi energy $E_F \sim t_a$ is known.

More recently, an apparent third angular effect was detected in a-b plane rotations in $(TMTSF)_2X$ [$X=ClO_4$ (Ref. 7) and PF_6 (Ref. 8)], and perhaps in $(DMET)I_3$.[9] The main feature of this effect is the appearance of a single kink in the interlayer magnetoresistance as a function of angle when the field is rotated in the most conducting a-b plane. The authors of Ref. 7 proposed an explanation based on the appearance of closed orbits on the face of the quasi-one-dimensional open Fermi surface (FS), and supported their conjecture with conductivity calculations which reproduce a kink in $\rho_{zz}(\phi)$. This notion of closed vs open orbits had in fact been brought up previously in the context of these materials by Danner and co-workers.[6] However, in Ref. 7, a satisfactory match between calculation and experiment (i.e., similar angles for the kink) was obtained only after underestimating band parameters. It was recently pointed out by Lebed' and Bagmet[10] that closed orbits may not be relevant for this third effect when realistic band parameters are used (i.e., when $t_b \gg t_c$). Instead, they suggested the origin lies in the role of ''effective electrons'' at inflection points (IP's) on the warped, open FS.

In this paper, we show by detailed calculation and experiment on $(TMTSF)_2PF_6$ at 8.3 kbar that the third angular effect is in fact due to the velocity-preserving nature of these effective electrons via their proximity to geometrical inflexion points on the FS. The role of closed orbits, which indeed exist for a small angular regime, is more closely associated with the ambient magnetoresistance, and plays essentially no role in the formation of the most obvious observable feature of the third effect, the kink in $\rho_{zz}(\phi)$. All of the main features of our measured resistivity are reproduced in simulations invoking classical Boltzmann transport, suggesting that Fermi liquid theory works at this pressure, in apparent contrast to a report of non-Fermi liquid behavior at higher pressure,[11] but in agreement with a recent analysis[12] of ρ_{xx} data at similar pressures. Our analysis is likely applicable to some quasi-two-dimensional BEDT-TTF molecular conductors as well, where Lebed'-like features are purported to arise due to open orbits, and where peak structure in angle-dependent magnetoresistance experiments was recently reported to result from closed orbits.[13]

Planar TMTSF molecules form highly conducting chains along the a axis, with these chains molding a-b planes separated by an anion layer ($X=PF_6$, ClO_4, NO_3, etc.) along the c direction. This structure yields a nearly one-dimensional FS consisting of a pair of warped sheets at $k_x \approx \pm k_F$. The warping is parametrized by hopping integrals t_i for which bandwidths are estimated from numerous experiments and calculations to be in the ratio $4t_a:4t_b:4t_c \approx 1\ \text{eV}:0.1\ \text{eV}:0.003\ \text{eV}$.[14] In this work, a single-crystal sample of $(TMTSF)_2PF_6$ was mounted inside a miniature pressure cell[15] tuned to 8.3 kbar. The sample assembly was then mounted on a rotary cryostat in a horizontal magnet, with internal and external rotators providing dual axis rotation (θ,ϕ). The interlayer resistance $R_{zz}(\phi)$ for various values of θ at fixed T and H was monitored using 1 μA current. That is, we rotated from a to b with and without a field component along the c direction. In doing so, we were able to test the effects of closed orbits and inflection points.

Our main experimental result is shown in Fig. 1, at 7 T and 0.32 K, as a series of rotations from the a-c plane to the b-c plane (offset for clarity). The angles ϕ and θ are measured from the a-axis and the a-b plane, respectively. The bottom trace has zero tilt along c, and so is a pure a-b rotation. A pair of distinctive kinks forming local minima are observed at $\phi = \pm 18.5°$. This is the ''third angular effect.''

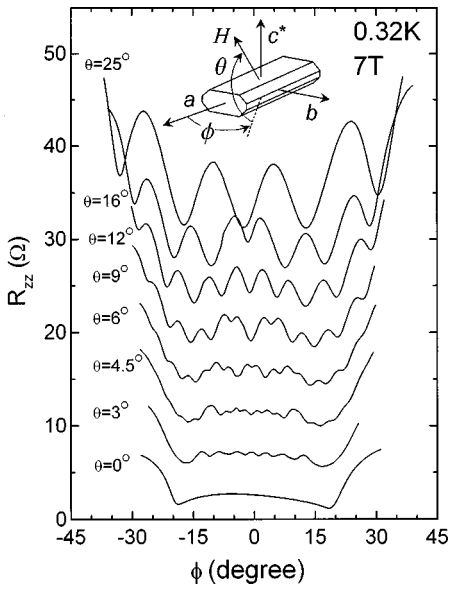

FIG. 1. Angle dependence of the interlayer resistance in $TMTSF_2PF_6$ for various tilts θ out of the a-b plane. The third angular effect, seen most clearly in the pure a-b rotation at $\theta=0°$, persists for finite θ, where Lebed'-like oscillations emerge.

The other traces have varying field tilts along c. There are two features of note: the main set of local minima near $\phi=18°$ persists for all tilts θ, and a series of AMRO appears for finite θ, growing in size with increasing θ. The angular positions of all the AMRO peaks and valleys are independent of both temperature and field strength, suggesting that they are associated with the FS topology.

Recently, Osada and co-workers[7] interpreted a similar a-b plane kink in $(TMTSF)_2ClO_4$ as due to electron orbits changing from closed to open as ϕ is increased, at a critical angle $\phi_c=\tan^{-1}(2t_b b/\hbar v_F)$. We submit that this formula does not describe the open-closed angle, but rather the inflection angle at which the external field is aligned normal to a tangent plane at an IP on the FS. Since the FS is corrugated with amplitudes $4t_b/\hbar v_F$ and $4t_c/\hbar v_F$ along k_x, the creation of the closed orbit relies on t_b/t_a as well as t_c/t_a. When $t_b \gg t_c$, as is the case for these quasi-one-dimensional systems, the angle ϕ_{CO} at which the closed orbit vanishes is in general quite different from the IP angle ϕ_{IP}. For example, for $t_a/t_b=8.5$ [appropriate for $(TMTSF)_2PF_6$] our simulations show that $\phi_{CO}\sim 6.5°$ for $t_b/t_c=30$, while the inflection angle is $\phi_{IP}=20.15°\pm 0.10°$, as we discuss later. While the difference between ϕ_{CO} and ϕ_{IP} can be smaller, unrealistic anisotropy ratios are required to get ϕ_{CO} up to 20°, something like $t_a/t_b\sim t_b/t_c\sim 4$. Using the velocity-velocity correlation function in a semiclassical treatment, electrons that form these closed orbits, initially near $(k_y,k_z)=(0,0)$ and $(\pi/b,\pi/c)$, can be shown to provide little or no contribution to the c-axis conductivity, since they have close to zero initial velocity along c.

Straightforward evidence against the role of closed orbits in the kink structure can be found when the orientation of the field has a third angular component, as in Fig. 1. Theoretically, a field tilt toward c as small as $\theta=1.1°$ eliminates all possibility of closed orbits anywhere on the FS. Thus, any features associated with closed orbits should disappear with a very small tilt. On the contrary, the local minimum near $\phi\sim 18°$ in Fig. 1 persists even with a considerable amount of θ tilt. To understand these features, the z-axis conductivity was calculated using a dispersion relation for a quasi-one-dimensional system with pair of sheetlike FS's:

$$E(k)=-2t_a\cos(k_x a/2)-2t_b\cos(k_y b)-2t_c\cos(k_z a/2) -E_F. \quad (1)$$

Here, $E_F=-\sqrt{2}t_a$ is the Fermi energy in a $\frac{1}{4}$-filled band, and a, b, and c are lattice constants. An electron in a magnetic field can be described by the equation of motion, $\hbar d\mathbf{k}/dt=e\mathbf{v}\times\mathbf{B}=e\mathbf{v}_k E(\mathbf{k})\times\mathbf{B}/\hbar$. Using the Boltzmann transport equation, the conductivity along $c\|z$ can be calculated as

$$\sigma_{zz}=(e^2/4\pi^3)\int d\mathbf{k}\tau v_z(\mathbf{k},t=0)\langle v_z(\mathbf{k},t)\rangle\partial f/\partial E. \quad (2)$$

Here f is the Fermi distribution function, a constant scattering time τ is assumed, and the average velocity is

$$\langle v_z(\mathbf{k})\rangle=\int_{-\infty}^{0}\frac{dt}{\tau}e^{t/\tau}v_z(\mathbf{k},t). \quad (3)$$

The resistivity $\rho_{zz}=1/\sigma_{zz}$ was calculated by solving Eq. (2) numerically for 1681 initial momentum states on the FS (i.e., 41×41 sites) and integrating numerically the velocity-velocity correlation function over the FS. A ''stiff Gear'' algorithm was used to solve the differential equation in which each momentum state k_x, k_y, and k_z evolves with a different rate over time. We used an orthorhombic approximation to the true triclinic structure, with lattice constants $a=6.980$, $b=7.581$, and $c=13.264$ Å, reported for PF_6 at 7 kbar and 1.7 K.[16] The band parameters employed, $t_a/t_b=8.5$, $t_b=0.0311$ eV, $t_b/t_c=60$, and $\tau=6.3\times 10^{-12}$ s, were determined from a-c plane rotations on the same sample,[17] in the manner of Ref. 6. The role of the inflection angle in σ_{zz} was examined by numerically solving the dispersion relation (1) for k_x. The inflection angles on the warped FS (see Figs. 2 and 3), measured between the a axis and the normal to the tangent plane at the IP, have both θ and ϕ components, as detailed in Fig. 2(c) for $t_b/t_c=30$. Notice that for a pure a-b rotation ($\theta=0$), there are two possible inflection angles, one near $\phi=20.05°$ and the other at $\phi=20.25°$.

In order to describe the roles of inflection angles and closed orbits, we show in Fig. 2 the calculated angular dependence of the time-averaged velocity $\langle v_z(k,t)\rangle$ for electrons initially located at various points on the FS when the field was turned on. When the field is aligned at an inflection angle, electrons in the vicinity of the IP near $(\pi/2b,\pi/2c)$ *preserve in time their initial z-axis velocity*, and thus dominate the conductivity. These electrons exhibit a peak in $\langle v_z\rangle$ near $\phi_{IP}\sim 20°$, and become very effective, even if they do not lie on the IP line in the inset to Fig. 2(c). This is shown in Fig. 2(a) for electrons 1 and 2, with initial momentum components at and away from, respectively, the point $(k_y,k_z)=(\pi/2b,\pi/2c)$. Electron 1 is at $(k_y^*,\pi/2c)$, and electron 2 at $(k_y^*,0.7\pi/c)$. Here, k_y^* is very nearly, but not exactly, $\pi/2b$. For such pure a-b plane rotations, electron 3 near another IP at $(k_y^*,\pi/c)$ will give no contribution to the conductivity at $\phi_{IP}\sim 20°$, for it has zero average velocity

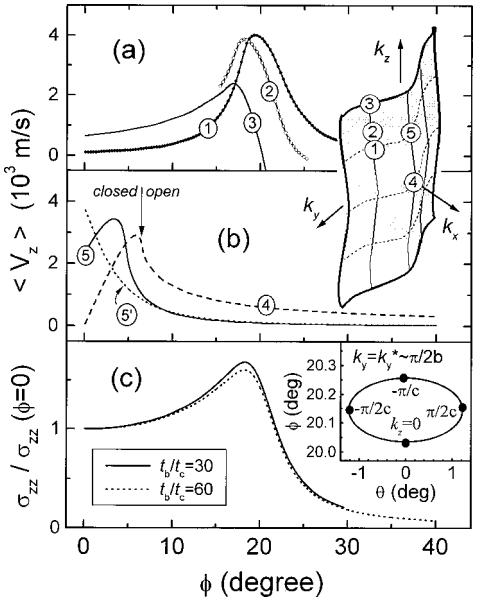

FIG. 2. Calculated angle dependence of velocity for open-orbit electrons at various points on the Fermi surface, for $B=7$ T and $t_b/t_c=30$ (ϕ is measured from k_x to k_y). In (a), trace 1 represents an effective electron at inflection point $(k_y,k_z)=(k_y^*,\pi/2c)$, with $k_y^* \approx \pi/2b$. Electron 2 at $(k_y^*,0.7\pi/c)$, though not at the IP, also becomes effective. Electron 3 starts at an IP at $(k_y^*,\ \pi/c)$, but is less effective, since $\langle v_z \rangle$ passes through zero. In (b), electron 4 at (0,0) has a closed orbit only out to $\phi=6.5°$; likewise for electron 5 at $(0,\pi/2c)$ to 4.5°. If the field is tilted $\theta=1.2°$ toward k_z, all closed orbits vanish, as seen in trace 5′, which is electron 5 in the tilted field. Panel (c) shows the full conductivity. Notice that the closed orbits produce no discernable features in $\sigma(\phi)$, while the effective electrons yield the peak at $\phi=18.3°$. Also shown is $\sigma(\phi)$ for $t_b/t_c=60$, and the allowed angular range of inflection points for $k_y=k_y^*$.

there, *and is therefore ineffective* with regard to the 3rd angular effect; likewise for electrons at $(k_y^*,0)$. In this regard, our analysis differs from that of Ref. 10, which had electrons near these latter two IP's being most effective. We remind the reader that, with $\theta=0°$, the field has no possibility of aligning normal to the IP tangent plane for the electrons near site 1 [refer again to the inset in Fig. 2(c)]. However, their proximity to this IP makes these electrons effective still, and creates a peak in $\langle v_z \rangle$ at an angle smaller than the actual IP angle. This explains why the full conductivity peak in Fig. 2(c) occurs below the actual inflection angle, consistent with our data in Fig. 1.

When the field is aligned along the a axis ($\theta=\phi=0$), highly symmetric closed orbits form at $(k_y,k_z)=(0,0)$ and $(\pi/b,\pi/c)$, with average velocity zero as shown for electron 4 at $\phi=0$ in Fig. 2(b). As the field is tilted away from a, this orbit becomes elongated along k_y and develops positive average velocity. Finally, the orbit becomes open and stretches along k_z at the critical angle $\phi_c=6.5°$, just past the peak in trace 4 as indicated. Near another effective electron site at $(0,\pi/2c)$, the electron trajectory stretches across many Brillouin zones (BZ's) along k_z while covering a small portion of one zone along k_y, for a small tilt ϕ. For such electrons, exemplified by trace 5 in Fig. 2(b), all closed orbits vanish by $\phi=4.5°$. These orbits provide peaks in $\langle v_z \rangle$ toward $\phi=0$, and without them the angular dependence would follow trace 5′, which is the dependence of electron 5 with a field tilt toward k_z of $\theta=1.2°$. This demonstrates that electrons at different locations on the FS become effective in different orientations, as the field is swept away from the a axis—electrons near $(0,\pm\pi/2c)$ become effective with a small tilt while those near $(\pm\pi/2b,\pm\pi/2c)$ will shape the conductivity near the inflection angle. Since the position of the dip in the measured resistance is sensitive to the bandwidth ratio t_a/t_b, as are the primary peaks in the a-c resonance, very accurate estimations of this ratio can be made. One point we would like to stress here is that competition between effective electrons on different sections of the FS is responsible for all aspects of the magnetoresistance, including that at angles far from any inflection angle.

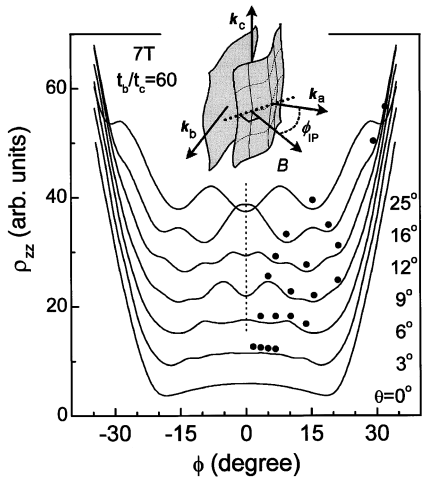

FIG. 3. Calculated resistivity at 7 T, $t_b/t_c=60$, for several tilt angles (offset) as in Fig. 1. The third angular effect, reproduced in the minimum at $\pm\phi=18.3°$ for $\theta=0°$, persists for finite tilt θ, where new oscillations develop. The dots represent angles where Lebed' minima are calculated to occur.

Adding up the contributions from all sampled electrons across the FS yields the total conductivity σ_{zz}, Fig. 2(c), and hence the resistivity ρ_{zz}, shown in Fig. 3. Close similarity can be found between theory (Fig. 3) and experiment (Fig. 1), starting with the pure a-b rotation. In the calculated result, the main minimum is found at $\phi_0=18.3°$, close to our experimental observation of $\phi_0=18.5°$ (recall that the parameters which yielded the calculated value are consistent with a-c rotation experiments, Ref. 17). When the a-b rotations have a third field component, rich oscillations appear in addition to the kink of the third effect, again similar to data in Fig. 1. We can test whether the Lebed' resonance plays a role in the oscillations in Figs. 1 and 3. The calculated positions for magic angle minima appear as dots in Fig. 3, for commensurability ratio p/q up to 4, using $\tan\alpha=(p/q)(b/c)$, with α measured from c to b.[2,3] There is strong correlation between these positions and the minima in the calculation. We can also recast the measured a-b rotations with finite tilt in Fig. 1 as projections onto the b-c plane, using $\tan\alpha=\sin\phi/\tan\theta$, as shown in Fig. 4. Magic angles $p/q=0-9$ are shown by the dotted lines. The resistance dips line up very well with the magic angles, such that the Lebed' description seems convincing. Thus, a mixed dispersion term is not required to reproduce this effect, in contrast to previous reports.[5] It seems that the Lebed' effect can

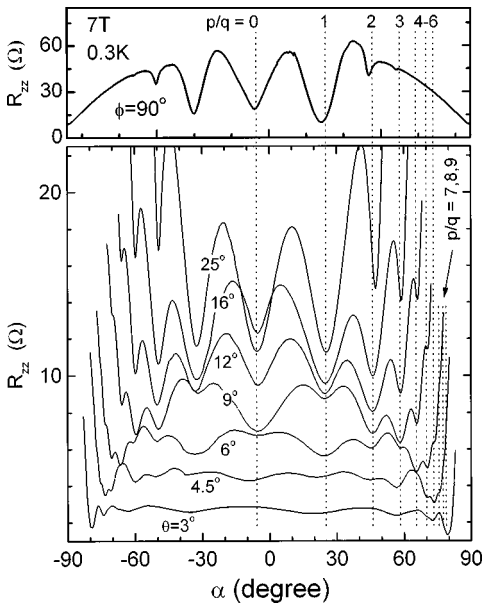

FIG. 4. Data of Fig. 1 replotted vs b-c plane angle α, via $\tan\alpha=\sin\phi/\tan\theta$. Magic angles up to commensurability ratio $p/q=9$ are indicated. At the top is a conventional b-c rotation, with minima observed only up $p/q=3$.

be explained and modeled with the conventional, simple band structure of Eq. (1), at least when one calculates the conductivity in rotations *out of* the b-c plane. A puzzling situation still exists, however, as it appears that the magic angle resonances are still not reproduced in calculations for rotations in the plane, where the effect is thought to be strongest.

The normal configuration for observing the Lebed' effect appears in Fig. 4(a). Interestingly, many more minima appear in the off-axis data of Fig. 4(b) than in this direct b-c rotation. Our simulations show that for ϕ rotations with finite θ, electron motion becomes distorted and asymmetric, with an electron's path covering one side of the BZ much more than the other as the magic angle index p/q increases. If one invokes Chaikin's hot spot scenario[18] and locates a region in the BZ where electron-electron scattering is enhanced, an electron at a high magic angle is able to cross the hot spot less often than one at a lower magic angle. The one with reduced chance of crossing the hot spot is more likely to result in a resistance dip. While this may play a role in explaining why we detect more magic angles in off-axis, as compared to on-axis, rotations (Fig. 4), it is not yet clear that the mechanism can be justified.[19]

In summary, we have demonstrated theoretically and experimentally that ''effective electrons'' on different sections of a quasi-one-dimensional Fermi surface are responsible for the so-called third angular magnetoresistance effect. Closed orbits play a minimal role, contributing only to the background near $H\|k_x$. Rich oscillations observed in out-of-plane rotations were reproduced in calculations and associated with the Lebed' effect. The theoretical aspect was done entirely within Fermi-liquid theory.

This research was supported by the National Science Foundation, under Grant No. DMR-9258579. We would like to thank T. Osada and A. G. Lebed' for beneficial communications and E. Chashechkina and P. M. Chaikin (DMR-9510246) for use of the pressure cell.

*Present address: Department of Physics, Princeton University, Princeton, NJ 08544.

†Electronic address: naughton@acsu.buffalo.edu

[1] I. J. Lee, M. J. Naughton, G. M. Danner, and P. M. Chaikin, Phys. Rev. Lett. **78**, 3555 (1997).

[2] A. G. Lebed', Pis'ma Zh. Eksp. Teor. Fiz. **43**, 137 (1986) [JETP Lett. **43**, 174 (1986)].

[3] M. J. Naughton *et al.*, in *Advanced Organic Solid State Materials*, edited by J. W. Fleming, G. H. Sigel, S. Takahashi, and P. W. France, MRS Proceedings No. 173 (Materials Research Society, Pittsburgh, 1990), p. 257.

[4] T. Osada, A. Kawasumi, S. Kagoshima, N. Miura, and G. Saito, Phys. Rev. Lett. **66**, 1525 (1991); M. J. Naughton, O. H. Chung, M. Chaparala, X. Bu, and P. Coppens, *ibid.* **67**, 3712 (1991).

[5] T. Osada, S. Kagoshima, and N. Miura, Phys. Rev. B **46**, 1812 (1992); A. Lebed', J. Phys. I **4**, 351 (1994).

[6] G. M. Danner, W. Kang, and P. M. Chaikin, Phys. Rev. Lett. **72**, 3714 (1994).

[7] T. Osada, S. Kagoshima, and N. Miura, Phys. Rev. Lett. **77**, 5261 (1996).

[8] M. J. Naughton, I. J. Lee, P. M. Chaikin, and G. M. Danner, Synth. Met. **85**, 1481 (1997).

[9] H. Yoshino *et al.*, J. Phys. Soc. Jpn. **64**, 2307 (1995).

[10] A. G. Lebed' and N. N. Bagmet, Phys. Rev. B **55**, 8654 (1997).

[11] G. M. Danner and P. M. Chaikin, Phys. Rev. Lett. **75**, 4690 (1995).

[12] L. P. Gor'kov and M. Mochena (unpublished).

[13] N. Hanasaki, S. Kagoshima, T. Hasegawa, T. Osada, and N. Miura, Phys. Rev. B **57**, 1336 (1998).

[14] C. S. Jacobsen, D. B. Tanner, and K. Bechgaard, Phys. Rev. B **28**, 7019 (1983); P. M. Grant, J. Phys. Colloq. **44**, C3-847 (1983).

[15] G. M. Danner and P. M. Chaikin, Rev. Sci. Instrum. **66**, 3951 (1995).

[16] B. Gallois *et al.*, Mol. Cryst. Liq. Cryst. **148**, 279 (1987).

[17] I. J. Lee and M. J. Naughton (unpublished).

[18] P. M. Chaikin, Phys. Rev. Lett. **69**, 2831 (1992).

[19] A. T. Zheleznyak and V. M. Yakovenko, Synth. Met. **70**, 1005 (1995).